Appl. Phys. B 49, 155–161 (1989)

Applied Physics B Photophysics and Laser Chemistry

NaK $2^1\Sigma^+ \rightarrow 1^1\Sigma^+$ Band Optically Pumped Laser Near 1.02 μm

B. K. Clark*, W. T. Luh, and J. Huennekens

Department of Physics, Lehigh University, Bethlehem, PA 18015, USA

Received 8 December 1988/Accepted 1 March 1989

Abstract. Optically pumped laser emission has been observed on the NaK $2(A)^1\Sigma^+ \rightarrow 1(X)^1\Sigma^+$ electronic state transition. The emission occurs between 1.015 and 1.035 μm when a sodium-potassium heat-pipe oven is pumped with 695–745 nm pulsed dye laser radiation. The laser emission occurs on many ro-vibrational transitions without the use of cavity mirrors. However, the addition of a simple cavity increases both the number of observed lasing transitions and the amplitude of the emission on each line. We report our results for the dependence of the emission intensity on pump laser power, oven temperature, and buffer gas pressure.

PACS: 42.55.Hq, 33.50.Dq

Optically pumped lasers (OPL's) based upon electronic transitions in alkali diatomic molecules were first demonstrated in sodium vapor by Henesian et al. in 1976 [1]. This pulsed alkali OPL was soon followed by a report of continuous laser action on the Na_2 $B \rightarrow X$ band [2]. Since that time, various studies have produced OPL emission based upon the $A \rightarrow X$ and $B \rightarrow X$ bands of the homonuclear alkali molecules Li_2, Na_2, and K_2 [3–14]. OPL emission from more highly excited states of the sodium molecule has also been observed [15–18]. Of particular interest to the present study, OPL emission has been observed from the heteronuclear alkali molecule NaRb [19]. These alkali OPL's have now been made to operate on a large number of fixed frequency lines in the range 400–910 nm as well as on several lines in the 2.5 μm region. Other dimers such as Bi_2, S_2, Te_2, and I_2 have also been made to yield stimulated emission in the visible and near-infrared regions through OPL transitions. Such lasers have applications in gain modulated spectroscopy [20] and in the determination of electronic transition moments [21].

Optically pumped alkali lasers may be treated as three level lasers as is shown in Fig. 1. In general, two mechanisms are responsible for the OPL emission. In the first, a thermally populated level of the ground electronic state is pumped on-resonance in an allowed ro-vibrational transition to the upper laser level. Lasing then occurs to thermally unpopulated high lying levels of the ground state. The second mechanism is a Raman process where the excitation and emission wavelengths can be either resonant or slightly off resonant with the same three levels. This Raman process leads to asymmetric gain favoring emission parallel to the direction of the pump laser propagation [4, 22].

In the present work we report laser emission on NaK $2^1\Sigma^+ \rightarrow 1^1\Sigma^+$ electronic transitions. The observed OPL lines consist of P and R transitions originating from vibrational levels in the range $v' = 17$–33 of the $2^1\Sigma^+$ electronic state and terminating on the $v'' = 36$–53 levels of the $1^1\Sigma^+$ ground state. The initial levels that are excited by the pump laser are the thermally populated ro-vibrational levels of the $1^1\Sigma^+$ state ($v'' = 0$–7). With the high gain that is obtained using a high-power, pulsed dye laser as the excitation source, lasing (or more correctly amplified spontaneous emission) can be observed on many lines without the use of cavity mirrors. However, the addition of a simple cavity increases both the number of lasing transitions and the amplitude of each emis-

* Present address: Dept. of Physics, Illinois State University, 311 Moulton Hall, Normal, IL 61761, USA

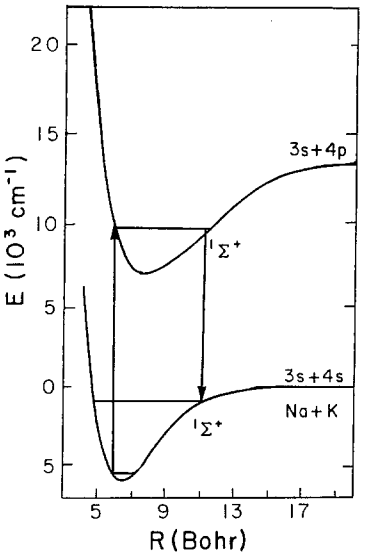

Fig. 1. Schematic potential energy level diagram for the NaK molecule showing the observed OPL transitions. The arrow pointing up represents the pumping process from low lying levels of the $1^1\Sigma^+$ state to various levels of the $2^1\Sigma^+$ state. The downward arrow represents OPL emission from the pumped level to initially unpopulated, high-lying levels of the $1^1\Sigma^+$ state

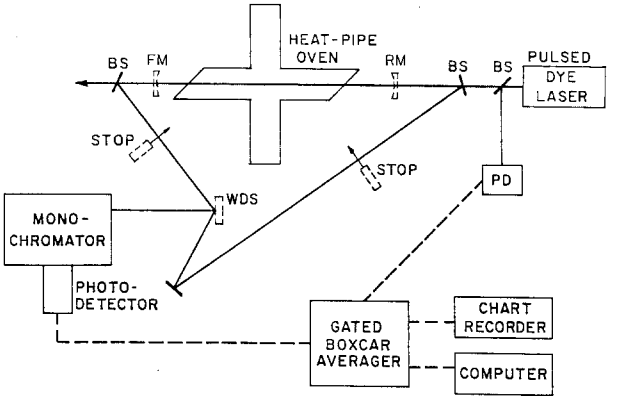

Fig. 2. Experimental set-up. Here PD, BS, RM, FM, and WDS represent photodiode, beam splitter, rear cavity mirror, forward cavity mirror, and white diffusing surface, respectively

sion line. While the lasing transitions reported here are similar to the other alkali OPL's, the present observations represent only the second case of OPL emission involving the heteronuclear alkali molecules and the first such observation in the NaK molecule. In addition, the present work extends the known alkali dimer laser emissions into the 1.0 μm region.

1. The Experiment

The experimental apparatus is shown in Fig. 2. A vapor consisting of a mixture of sodium and potassium was contained in a 4-way cross, stainless-steel, heat-pipe oven. The initial mixture of potassium and sodium was ~2:1 although temperature cycling and subsequent reloadings caused the ratio of potassium to sodium atoms in the vapor phase to vary with time. The oven also contained argon buffer gas which was varied in pressure over the range 1–130 mbar. Since the oven was typically not operated in the heat-pipe mode, the temperature could be independently varied from ~400–600 °C. To verify the molecular species involved in the OPL process, a second heat pipe, containing pure potassium vapor, could be substituted for the Na–K oven.

The Na–K vapor was pumped by a dye laser which was in turn pumped by a frequency doubled, pulsed Nd:YAG laser. Calibration of the dye laser frequency was carried out using the optogalvanic effect in a neon-filled hollow cathode lamp. We used the dye LDS 722, which tunes over the range 690–760 nm. However, most of the OPL pumping occurred between 695 and 745 nm. The peak power of the dye laser was ~1 MW in this range. The dye laser beam was either unfocused or weakly focused into the heat-pipe oven.

Emission from the Na–K oven directed generally parallel or antiparallel to the pump beam (referred to as forward and backward emission, respectively) could be monitored by the use of beam splitters which directed the beams to a white diffusing surface placed in front of a monochromator. Light passing through the monochromator was detected with a liquid nitrogen-cooled, intrinsic germanium detector. In all cases, appropriate color filters were used to eliminate second and higher order diffraction from the monochromator grating, as well as unwanted pump laser light. The detector output was then processed by a boxcar-averager and sent to both a chart recorder and a computer for later analysis. With this setup, only stimulated emissions from the oven could be detected since no focusing optics were employed along their optical paths.

The relative forward to backward detection efficiencies were calibrated with the oven cold by first aligning the forward detection optics and then retroreflecting the pump laser beam upon itself and through the backward detection optics. A beam splitter was used in the backward path as shown in Fig. 2, while either a beam splitter (for roughly equal forward to backward efficiencies) or a mirror (for higher sensitivity) was used in the forward direction. With this calibration of the forward to backward efficiencies, we could determine the relative forward to backward OPL intensity ratio. Finally, for the highest sensitivity the white diffusing surface was sometimes bypassed, and the stimulated emission sent directly into the monochromator using highly-reflective mirrors.

Under these conditions, neutral density filters were needed to regulate the light levels.

Normally the 0.75 m monochromator was set to pass light at a specific wavelength in the 1.015–1.035 μm region with a bandpass of 0.3–6.7 nm. For laser excitation scans, the monochromator slits were set to 3 mm (yielding a spectral resolution of 6.7 nm) and the laser frequency was scanned. With the laser linewidth of ~ 0.1 cm^{-1}, well defined rotational-vibrational progressions could be observed.

The power dependence of the OPL emission at 1.02 μm was determined using a series of neutral density filters which were calibrated in place using a photodiode (see Fig. 2). By referencing the stimulated emission intensity at 1.02 μm to the pump laser intensity and taking account of the relative efficiency of the intrinsic germanium detector at the two wavelengths, the conversion efficiency of this OPL emission could be determined. The relative efficiency of the detection system at the pump laser and OPL wavelengths was determined following the procedures outlined in [23] utilizing a tungsten halogen lamp with known relative emission vs. wavelength.

Most of the studies were carried out without the use of OPL cavity mirrors. However, several cavity designs were tried in attempts to enhance the OPL emission. In all cases the rear cavity mirror was chosen to have a 3 m radius of curvature, >99% reflectivity at 1.02 μm and >80% transmission between 700 and 800 nm. Several forward cavity mirrors were tried. The first was ~50% reflecting at 1.02 μm and >80% transmitting between 700 and 800 nm, with a 3 m radius of curvature. The second was a flat quartz window with one side antireflection coated. Its effective reflectivity was ~5%. The third was a plane sapphire window with a reflectivity of ~7% from each surface.

Laser excitation scans were made without any cavity mirrors and for each forward cavity mirror (including the case of no forward reflector) in conjunction with the rear high reflector. The dependence of the 1.02 μm emission on pump laser power was measured with the sapphire window cavity and with no cavity present. The effect of each cavity configuration on the intensity of selected lasing transitions was studied by misaligning and then realigning each mirror to its optimal position.

2. Results and Discussion

The forward emission at 1.02 μm was first observed when we heated the Na–K heat-pipe oven above 500 °C at ~50 mbar buffer gas pressure during studies of parametric wave-mixing and other coherent emissions [24]. With the monochroamtor set to specific wavelengths near 1.02 or 1.03 μm, we obtained laser

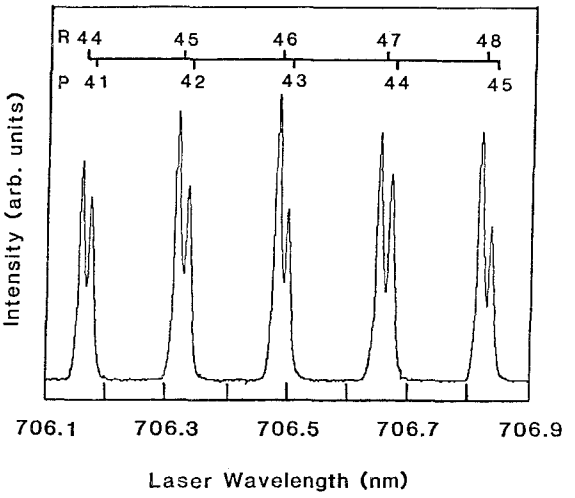

Fig. 3. Laser excitation spectrum corresponding to OPL emission at 1.021 μm (monochromator bandpass ~1.4 nm). The labelled *P* and *R* absorption lines are part of the $2^1\Sigma^+(v'=28) \leftarrow 1^1\Sigma^+(v''=0)$ band. The heat-pipe oven was operated at 519 °C with an argon buffer gas pressure of 50 mbar

excitation scans which show ro-vibrational progressions corresponding to *P* and *R* line absorptions on the NaK $2(A)^1\Sigma^+ \leftarrow 1(X)^1\Sigma^+$ band (Fig. 3). Most of the observed transitions originate from low lying vibrational levels of the ground state. The upper state vibrational level ranges from $v'=17$–33.

The 1.02–1.03 μm OPL emission detected by the germanium detector is the $2^1\Sigma^+ \rightarrow 1^1\Sigma^+$ downward transition to initially unpopulated, high-lying levels of the ground state ($v''=36$ to 53). Due to the very high density of absorption lines leading to OPL emission in the vicinity of 1.03 μm (which is near the long-wavelength satellite of the NaK $2^1\Sigma^+ \rightarrow 1^1\Sigma^+$ band), we did not attempt to carry out a detailed identification of the lines in the spectrum. However, using the accurate experimental constants for the NaK $1^1\Sigma^+$ and $2^1\Sigma^+$ states from [25, 26], respectively, we were able to assign individual ro-vibrational absorption lines in the relatively simple region of the spectrum between 700 and 715 nm. Note that K_2 could be ruled out as the source of the OPL emission by the fact that no such emission was observed when pumping pure potassium vapor in this spectral range under similar conditions. Na_2 could also be eliminated since there are no Na_2 emission bands in the 1.02–1.03 μm region.

Using the 0.75 m monochromator with a fixed pump wavelength and 100 μm slits (0.3 nm resolution), the OPL emission near 1.02 μm could be resolved into an $R(J-1)$ and $P(J+1)$ doublet of one vibrational transition of the $2^1\Sigma^+ \rightarrow 1^1\Sigma^+$ band. The specific case of $J=49$, pumped via the

$$2^1\Sigma^+(v'=28, J'=49) \leftarrow 1^1\Sigma^+(v''=0, J''=48)$$

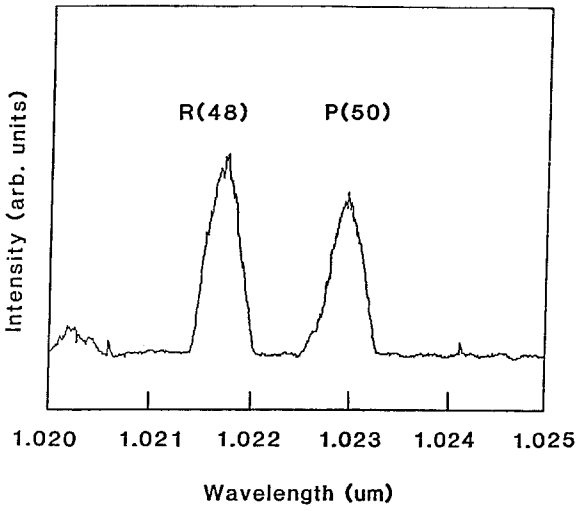

Fig. 4. Monochromator scan of the OPL emission with the pump laser tuned to the

$2^1\Sigma^+(v'=28, J'=49) \leftarrow 1^1\Sigma^+(v''=0, J''=48)$

transition. The oven temperature was 517°C, and the buffer gas pressure 33 mbar. The monochromator slits were set to give a resolution of 0.3 nm. This spectrum was taken using the high reflecting back cavity mirror and the sapphire window as the forward mirror. The weak line observed at 1.0202 μm has not been identified, but probably represents a weaker pumping from some higher level of the ground state $[1^1\Sigma^+(v''>0)]$. The separation of the two main peaks is in agreement with the energy splitting of the $v''=46$, $J''=48$ and 50 levels of the ground state. The observed OPL wavelengths and calculated Franck-Condon factors (see text) are also consistent with the interpretation that this OPL emission represents a single P, R doublet terminating at $1^1\Sigma^+(v''=46)$

transition is shown in Fig. 4. The observed emission peak positions are in agreement with those predicted for the

$2^1\Sigma^+(v'=28, J'=49) \rightarrow 1^1\Sigma^+(v''=46, J''=48, 50)$

lines from the constants of [25, 26]. (Note that although the $v''=0 \rightarrow v'=28$ band was by no means the most effective at producing OPL emission, it occurs in a relatively simple region of the spectrum where individual line assignments were possible. Consequently, much of our subsequent data analysis, such as power dependences and cavity studies, were carried out using lines of this band.)

Longer monochromator scans indicate that, with our level of sensitivity, each upper level pumped by the laser will, in general, only produce stimulated emission on a single P, R doublet of one vibrational band. We presume that these are the transitions with the highest gain, which is determined by the relevant Franck-Condon factors. These were calculated using the computer program INTENSITY [27] and RKR potential calculated from the NaK $2^1\Sigma^+$ and $1^1\Sigma^+$ molecular constants of Ross et al. [25, 26]. In Table 1 we list the strongest downward transitions (as determined from these calculated Franck-Condon factors) for various upper state vibrational levels. For each of the bands that were investigated in detail, lasing was observed only on the vibrational transition from the pumped upper level that has the largest Franck-Condon factor. In a homogeneously broadened gain medium, the upper level population gets clamped at the threshold value for the transition with the largest gain [16, 28]. In the present case, we are dealing with a Doppler (and therefore inhomogeneously) broadened gain medium. However, it is possible that a similar population clamping mechanism may be responsible for this observation of lasing on only one vibrational transition. It is likely that in cases where Franck-Condon factors are nearly equal, lasing could be observed on more than one vibrational band from a single upper level. It is also probable that weaker vibrational bands could be made to lase with the addition of a tuning element to the cavity. However, this was not attempted in the present work.

Table 1. List of the strongest downward transitions of the NaK $2^1\Sigma^+ \rightarrow 1^1\Sigma^+$ band (defined by the Franck-Condon factors) for a given upper vibrational state v'. Only those bands which radiate most strongly in the 1.01–1.035 μm range are listed. These are the bands which are most likely to contribute to the observed OPL emission. Column three gives the Franck-Condon factor $q \equiv |\langle v'|v''\rangle|^2$ for each transition, while column four gives roughly the band center wavelength [defined by the wavelength of the $Q(50)$ line]. Here, the most probable rotational level is $\sim J=50$ for our experimental temperatures

v'	v''	q	λ[μm]
17	36	0.1921	1.0334
18	37	0.2070	1.0337
19	38	0.2257	1.0340
20	39	0.2471	1.0340
21	40	0.2682	1.0339
22	41	0.2837	1.0337
23	42	0.2851	1.0332
24	43	0.2628	1.0326
25	43	0.2236	1.0251
26	44	0.2702	1.0244
27	45	0.2912	1.0235
28	46	0.2651	1.0224
29	47	0.1848	1.0211
30	47	0.1427	1.0139
31	50	0.1689	1.0232
32	51	0.1259	1.0210
33	53	0.1259	1.0231

In Fig. 5 we present a plot of the total OPL emission, with the laser tuned to the

$2^1\Sigma^+(v'=28, J'=49) \leftarrow 1^1\Sigma^+(v''=0, J''=48)$

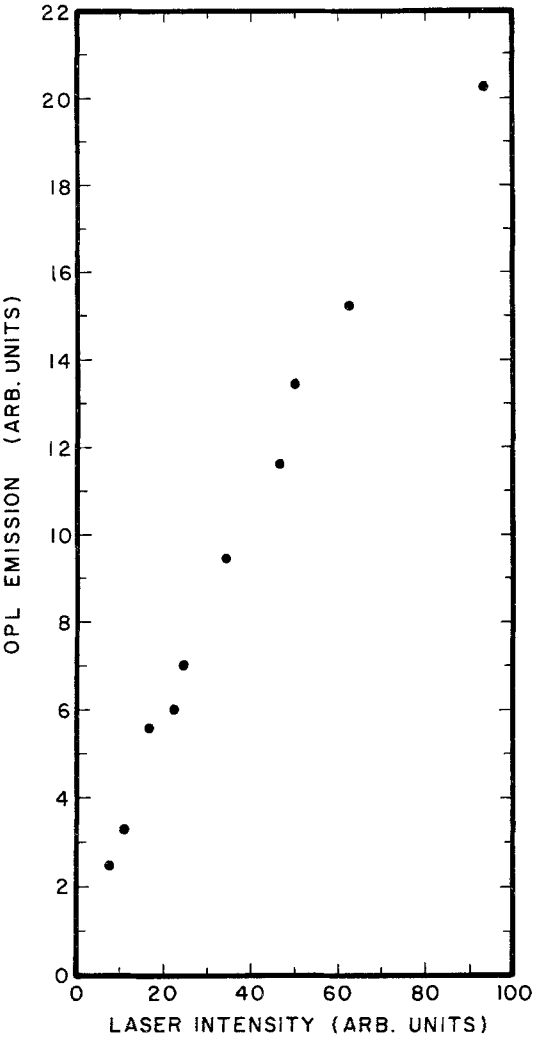

Fig. 5. OPL emission intensity as a function of pump laser power with the laser tuned to the $R(48)$ line of the $v''=0 \rightarrow v'=28$ transition. For these measurements, the oven temperature was 519 °C and the buffer gas pressure 35 mbar. The monochromator bandpass was 6.7 nm centered at 1.0224 μm. Laser power of 100 corresponds to the full available pump power (~1 MW). The pump laser beam was weakly focused to a diameter of ~0.1 cm in the oven. The sapphire window cavity was used for these data

transition, as a function of pump laser power. These data were taken with the sapphire window cavity in place. However, similar results were obtained without cavity mirrors. As can be seen for this relatively weak transition at fairly high pressure and temperature, the power dependence is roughly linear. However, other levels may show different power dependences due to saturation effects, etc. In particular, at lower temperatures (~460 °C) we observed not only saturation of some signals, but even reduced OPL emission as the laser power was increased to the highest levels. At lower laser power, all levels show the roughly linear power dependence seen in Fig. 5.

Using the sapphire window cavity and a monochromator bandpass of 6.7 nm, we found that the OPL emission could be produced by many absorption lines in addition to those clearly observed in the no-cavity case. Figure 6 shows a specific case in which the $v''=1$ to $v'=29$ absorption band can be seen overlapping the $v''=0$ to $v'=28$ band when the cavity is in place. These lines of the 1–29 band are very weak in the no-cavity spectrum. In some cases, bands which were very weak in the no-cavity case were enhanced by the cavity to intensities which were comparable to those of the strong bands.

Several other reflectors were tried as the forward cavity mirror. Use of either the quartz window, the 50% reflector, or no forward reflector at all resulted in essentially the same OPL emission as with the sapphire window. Strong lines (those observed clearly with no back reflector) generally only increased in intensity by ~10% with the use of a forward mirror. However, for these lines the back mirror and its alignment proved more critical, typically increasing the forward emission by a factor of ~2.5. For weak lines (those which were not observed clearly without a back reflector), the observed intensity typically increased by a factor of 4–6 with the addition of a forward cavity mirror.

The conversion efficiency of pump laser radiation to OPL emission was measured on the

$$2^1\Sigma^+(v'=28,\ J'=49) \rightarrow 1^1\Sigma^+(v''=46,\ J''=48)$$

transition following pumping from $v''=0, J''=48$ of the ground state. For these measurements, the heat-pipe oven temperature was 523 °C and the buffer gas pressure 40 mbar. The intensity of the laser beam passing through the heat-pipe oven was measured with the oven cold and hot. Then the intensity of the OPL emission was measured. The ratio of OPL emission to pump laser intensity transmitted through the cell was $\sim 10^{-4}$. Note that this conversion efficiency should be taken as only an order of magnitude estimate since it depends strongly on the buffer gas pressure, cell temperature, and vapor composition (see below). With no cavity present, we also measured a forward to backward intensity ratio of ~10:1.

For wavelengths in the range 700–720 nm, we found that the pump laser transmission through the oven at 515 °C and a buffer gas pressure of 50 mbar was ~50% of that observed with the oven cold. To test whether transmission of the pump laser beam through the heat-pipe oven was noticably reduced when pumping a transition giving rise to OPL emission, a beam-splitter was used to send a small amount of the transmitted pump laser radiation to a photodiode. A laser excitation spectrum, where the absorption of the pump laser radiation as measured by the photodiode was compared to OPL emission, showed no measur-

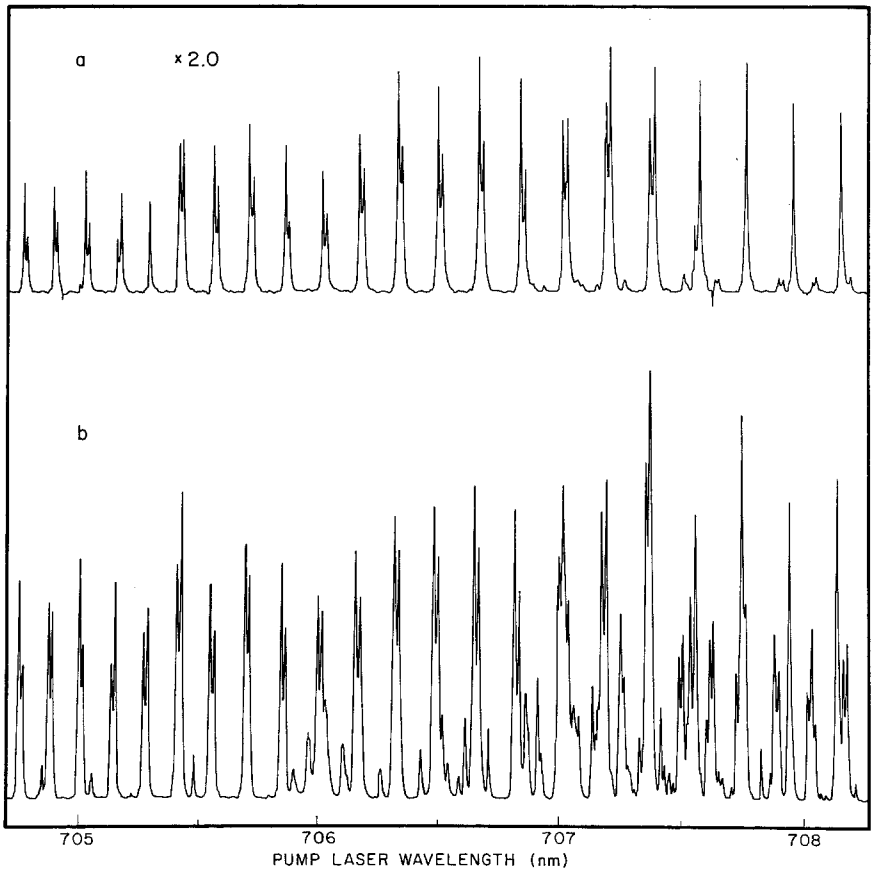

Fig. 6. **a** No OPL laser cavity and **b** sapphire window cavity laser excitation scans. The monochromator monitored emission at 1.022 μm with a resolution of 6.7 nm. The no-cavity scan clearly shows the $2^1\Sigma^+(v'=28) \leftarrow 1^1\Sigma^+(v''=0)$ ro-vibrational progression, while the sapphire window cavity scan shows in addition lines from the $2^1\Sigma^+(v'=29) \leftarrow 1^1\Sigma^+(v''=1)$ band. In both cases the buffer gas pressure was 35 mbar and the heat-pipe central temperature 515 °C

able decrease in the transmitted pump laser intensity specifically at the OPL absorption lines.

The observed OPL emission is a strong function of the vapor composition which is difficult to regulate in the mixed alkali oven. When the vapor is relatively rich in potassium, the most intense emissions are observed when pumping in the range 700–730 nm. At longer wavelengths the pump light is strongly absorbed in the oven, and the OPL emission is greatly reduced. We believe that a partial separation of the sodium and potassium vapors occurs in the oven and that the pump light can be absorbed by the K_2 $A^1\Sigma^+ \leftarrow X^1\Sigma^+$ band before reaching the region of greatest NaK density. Under such conditions, little or no NaK OPL emission can be seen for pump wavelengths greater than 740 nm despite the fact that the maximum of the NaK $2^1\Sigma^+ \leftarrow 1^1\Sigma^+$ absorption band lies in this region. With a more sodium rich mixture, the strongest OPL emissions are seen when pumping in the 720–745 nm region as one would expect from consideration of the NaK state constants and Franck-Condon factors.

Despite these composition dependent effects, we wanted to qualitatively investigate the temperature and buffer gas pressure dependence of the OPL emission for a fixed vapor mixture. This was carried out with a mixture relatively rich in potassium which was also used for the bulk of the other data. For a fixed buffer gas pressure of 33 mbar, we first observed OPL emission from the pumped level $2^1\Sigma^+(v'=28, J'=49)$ at 495 °C. The intensity increased until 548 °C when the heat pipe could no longer be operated at this fixed pressure. Note that at the lower temperatures studied here, the oven was not operating in the heat-pipe mode because the alkali vapor pressure was below that of the buffer gas. This resulted in mixing of buffer gas with the alkali in the central region of the oven. At higher temperatures, heat-pipe operation was established, resulting in an alkali vapor pressure equal to that of the buffer gas. In this regime, the central region of the oven contains only alkali vapor. When the power to the heaters was raised even further, the heat-pipe regime again broke down and vaporization of the alkali in the central region became so rapid that the pipe was soon occluded by alkali metal condensing near the ends of the wick.

Pumping the same ro-vibrational transition, the OPL emission as a function of buffer gas pressure was also studied at a fixed temperature of 515 °C. Under these conditions, the OPL intensity was greatest at 15 mbar and had almost disappeared by 60 mbar.

Pressures below 15 mbar could not be studied at this temperature because the pipe soon occluded due to a break down of the heat-pipe mode of operation.

The increase in OPL emission as temperature increased can probably be linked to the increasing number density of NaK molecules. We expect the signals to continue to increase with temperature until the pump beam attenuation becomes too severe. The decrease in OPL emission with increasing buffer gas pressure probably results from collisional excitation transfer out of the upper OPL level. It is possible that conversion efficiencies of 10^{-3} are achievable with this OPL system by further optimization of the buffer gas pressure, temperature, and cavity parameters.

3. Conclusions

In the present work we report observation of optically pumped laser emission in the region of 1.015–1.035 μm based upon $2^1\Sigma^+ \rightarrow 1^1\Sigma^+$ transitions of the NaK molecule. The large gain produced using high-power, pulsed laser excitation resulted in stimulated emission on many ro-vibrational transitions without the use of cavity mirrors. Under these conditions, we observed a forward to backward intensity ratio of $\sim 10:1$. The addition of a simple cavity (which contains no dispersing elements) increased the amplitude of these emissions and caused lasing to occur for many other $2^1\Sigma^+(v', J') \leftarrow 1^1\Sigma^+(v'', J'')$ absorptions which were below our detection limit in the no-cavity case. We investigated the dependences of the OPL emissions on cell temperature, buffer gas pressure, and pump laser intensity.

These results represent the first observation of OPL emission in the NaK molecule and demonstrate that alkali OPL's can be made to operate past 1.0 μm which, in the case of NaK, is near the $2^1\Sigma^+ - 1^1\Sigma^+$ band ($A-X$ band) satellite. The addition of a tunable cavity and further optimization of vapor parameters should result in laser action on many other lines in this spectral region.

Acknowledgements. The authors would like to thank the referees for several helpful comments and suggestions. This work was supported by the Army Research Office under grant DAALO3-86-K-0161, and the National Science Foundation under grant PHY-8451279.

References

1. M.A. Henesian, R.L. Herbst, R.L. Byer: J. Appl. Phys. **47**, 1515 (1976)
2. B. Wellegehausen, S. Shahdin, D. Friede, H. Welling: Appl. Phys. **13**, 97 (1977)
3. H. Itoh, H. Uchiki, M. Matsuoka: Opt. Commun. **18**, 271 (1976)
4. B. Welleghausen: IEEE J. QE-**15**, 1108 (1979)
5. B. Welleghausen: In *Metal Bonding and Interactions in High Temperature Systems*, ed. by J.L. Gole, W.C. Stwalley, ACS Symposium Series 179 (American Chemical Society, Washington, DC 1982) p. 461
6. C.N. Man-Pichot, A. Brillet: In *Metal Bonding and Interactions in High Temperature Systems*, ed. by J.L. Gole, W.C. Stwalley, ACS Symposium Series 179 (American Chemical Society, Washington, DC 1982) p. 487
7. A.R. Rajaei-Rizi, J.T. Bahns, K.K. Verma, W.C. Stwalley: Appl. Phys. Lett. **40**, 869 (1982)
8. P.L. Jones, U. Gaubatz, U. Hefter, K. Bergmann, B. Wellegehausen: Appl. Phys. Lett. **42**, 222 (1983)
9. J.T. Bahns, K.K. Verma, A.R. Rajaei-Rizi, W.C. Stwalley: Appl. Phys. Lett. **42**, 336 (1983)
10. W. Luhs, M. Hube, U. Schottelius, B. Wellegehausen: Opt. Commun. **48**, 265 (1983)
11. W. Luhs, B. Wellegehausen: Opt. Commun. **46**, 121 (1983)
12. C.N. Man, A. Brillet: J. Appl. Phys. **56**, 71 (1984)
13. W.T. Luh: Ph.D. Thesis, University of Iowa (1985)
14. W.T. Luh, J.T. Bahns, W.C. Stwalley: J. Mol. Spectrosc. **128**, 82 (1988)
15. B. Wellegehausen, W. Luhs, A. Topouzkhanian, J. d'Incan: Appl. Phys. Lett. **43**, 912 (1983)
16. P. Bernage, P. Niay, H. Bocquet: J. Mol. Spectrosc. **98**, 304 (1983)
17. Z.-G. Wang, Y.-C. Wang, G.P. Morgan, A.L. Schawlow: Opt. Commun. **48**, 398 (1984)
18. Z.G. Wang, H.R. Xia, L.S. Ma, Y.Q. Lin, I.S. Cheng: Appl. Phys. B **37**, 233 (1985)
19. V.M. Kaslin, O.F. Yakushev: Soviet J. Quant. Electron. **13**, 1575 (1983)
20. H.S. Schweda, G.K. Chawla, R.W. Field: Opt. Commun. **42**, 165 (1982)
21. J.B. Koffend, R. Bacis, R.W. Field: J. Chem. Phys. **70**, 2366 (1979)
22. U. Hefter, J. Eichert, K. Bergmann: Opt. Commun. **52**, 330 (1985)
23. R. Stair, W.E. Schneider, J.K. Jackson: Appl. Opt. **2**, 1151 (1963)
24. B.K. Clark, M. Masters, J. Huennekens: Appl. Phys. B **47**, 159 (1988)
25. A.J. Ross, C. Effantin, J. d'Incan, R.F. Barrow: Mol. Phys. **56**, 903 (1985)
26. A.J. Ross, R.M. Clements, R.F. Barrow: J. Mol. Spectrosc. **127**, 546 (1988)
27. (a) W.T. Zemke, W.C. Stwalley: Quant. Chem. Prog. Exch. Bull. **4**, 79–80 (1984); (b) K.M. Sando: Private communication
28. A. Yariv: *Introduction to Optical Electronics* (Holt, Rinehart and Winston, New York 1976) p. 171